BBA - Molecular Basis of Disease 1865 (2019) 1604–1616

Contents lists available at ScienceDirect

BBA - Molecular Basis of Disease

journal homepage: www.elsevier.com/locate/bbadis

LRP1 promotes synthetic phenotype of pulmonary artery smooth muscle cells in pulmonary hypertension

Marius M. Zucker[a], Lukasz Wujak[a], Anna Gungl[b], Miroslava Didiasova[a], Djuro Kosanovic[c,d], Aleksandar Petrovic[c], Walter Klepetko[e], Ralph T. Schermuly[c], Grazyna Kwapiszewska[b], Liliana Schaefer[f], Malgorzata Wygrecka[a,*]

[a] Department of Biochemistry, Universities of Giessen and Marburg Lung Center, Giessen, Germany
[b] Ludwig Boltzmann Institute for Lung Vascular Research, Medical University Graz, Graz, Austria
[c] Department of Internal Medicine, Universities of Giessen and Marburg Lung Center, Giessen, Germany
[d] Sechenov First Moscow State Medical University (Sechenov University), Moscow, Russia
[e] Department of Thoracic Surgery, Medical University of Vienna, Vienna, Austria
[f] Goethe University, School of Medicine, Frankfurt am Main, Germany

ARTICLE INFO

Keywords:
Pulmonary hypertension
Low density lipoprotein receptor-related protein 1
β1-integrin
Smooth muscle cell phenotype
Cell proliferation

ABSTRACT

Pulmonary hypertension (PH) is characterized by a thickening of the distal pulmonary arteries caused by medial hypertrophy, intimal proliferation and vascular fibrosis. Low density lipoprotein receptor-related protein 1 (LRP1) maintains vascular homeostasis by mediating endocytosis of numerous ligands and by initiating and regulating signaling pathways.

Here, we demonstrate the increased levels of LRP1 protein in the lungs of idiopathic pulmonary arterial hypertension (IPAH) patients, hypoxia-exposed mice, and monocrotaline-treated rats. Platelet-derived growth factor (PDGF)-BB upregulated LRP1 expression in pulmonary artery smooth muscle cells (PASMC). This effect was reversed by the PDGF-BB neutralizing antibody or the PDGF receptor antagonist. Depletion of LRP1 decreased proliferation of donor and IPAH PASMC in a β1-integrin-dependent manner. Furthermore, LRP1 silencing attenuated the expression of fibronectin and collagen I and increased the levels of α-smooth muscle actin and myocardin in donor, but not in IPAH, PASMC. In addition, smooth muscle cell (SMC)-specific LRP1 knockout augmented α-SMA expression in pulmonary vessels and reduced SMC proliferation in 3D *ex vivo* murine lung tissue cultures.

In conclusion, our results indicate that LRP1 promotes the dedifferentiation of PASMC from a contractile to a synthetic phenotype thus suggesting its contribution to vascular remodeling in PH.

1. Introduction

Pulmonary hypertension (PH) is a devastating disease characterized by a sustained elevation of pulmonary artery pressure and pulmonary vascular resistance. An impaired crosstalk between endothelial cells (EC) and smooth muscle cells (SMC) has been demonstrated to play a central role in PH pathogenesis. Endothelial cells, located on the inner layer of the blood vessels, influence the underlying SMCs, thereby regulating pulmonary arterial pressure and vascular resistance [1]. Upon injury and EC dysfunction, SMC undergo a “switch” from a contractile to a synthetic phenotype which is characterized by their excessive survival, proliferation, migration as well as production of extracellular matrix (ECM) components [2]. Increased deposition of ECM proteins and progressive stiffening of the vascular wall lead to the obliteration of pulmonary arteries, increased pulmonary vascular resistance and finally to right ventricular hypertrophy and failure [3]. Although, a number of biochemical and physical factors were found to modulate the SMC phenotype [1,2,4], the underlying molecular mechanisms are still not entirely understood.

The low density lipoprotein receptor-related protein 1 (LRP1) is a

Abbreviations: α-SMA, α-smooth muscle actin; EC, endothelial cell; ECM, extracellular matrix; FN, fibronectin; HOX, hypoxia; IPAH, idiopathic pulmonary arterial hypertension; LRP1, low density lipoprotein receptor-related protein 1; MCT, monocrotaline; MMP, matrix metalloprotease; NOX, normoxia; PASMC, pulmonary artery smooth muscle cell; PDGF, platelet-derived growth factor; PDGFR, PDGF receptor; PH, pulmonary hypertension; SMC, smooth muscle cell

* Corresponding author at: Department of Biochemistry, Faculty of Medicine, Universities of Giessen and Marburg Lung Center, Friedrichstrasse 24, 35392 Giessen, Germany.
E-mail address: malgorzata.wygrecka@innere.med.uni-giessen.de (M. Wygrecka).

https://doi.org/10.1016/j.bbadis.2019.03.012
Received 19 October 2018; Received in revised form 19 March 2019; Accepted 20 March 2019
Available online 22 March 2019
0925-4439/

multifunctional scavenger and signaling receptor. LRP1 internalizes, among others, proteases, protease-inhibitor complexes, ECM proteins, and growth factors [5]. Besides its role in endocytosis, LRP1 also functions as a signaling receptor. A number of cytosolic proteins were found to interact with the NPxY motifs in the cytoplasmic domain of LRP1 in order to transduce signals to the downstream effector molecules [6,7]. In addition, LRP1 was described to control intracellular signaling pathways by modulating the activity and cell surface abundance of other receptors. For example, the interaction of LRP1 with platelet-derived growth factor receptor (PDGFR) was shown to suppress PDGFR activation [6] and the association of LRP1 with β1-integrin was reported to control β1-integrin recycling and hence cell adhesion and migration [7].

In contrast to EC, the LRP1 is highly expressed in SMC [5]. It has the capacity to maintain vascular homeostasis by mediating the endocytosis of various ligands and by regulating signaling pathways. Deletion of the *LRP1* gene in vascular SMC was found to switch the cells to a synthetic phenotype consequently inducing SMC proliferation and migration. The underlying molecular mechanism appeared to rely on the ability of LRP1 to control the expression of proteases such as matrix metalloprotease (MMP) 9 and MMP2 and the activity of the PDGF-BB and the transforming growth factor-β signaling pathway [8]. Furthermore, LRP1 was shown to regulate inflammatory responses and to facilitate efferocytosis, a process by which apoptotic cells are removed by phagocytic cells, in the vascular wall [9] and to orchestrate vascular development by promoting recruitment of SMC and pericytes [10].

Although numerous studies have demonstrated the involvement of LRP1 in the development of vascular pathologies, its potential role in the regulation of PASMC activities with respect to the pathogenesis of PH has not yet been defined. Here, we demonstrate that LRP1 may control PASMC activities and thus contribute to vascular remodeling in PH.

2. Methods

2.1. Human material

The investigations were conducted in accordance with the Declaration of Helsinki principles and were approved by the local institutional review board and ethics committee. Informed consent was obtained from either the patients or their next-of-kin. Lung tissue was obtained from 24 IPAH patients who underwent lung transplantation at the Department of Cardiothoracic Surgery, Medical University of Vienna, Austria. Non-utilized donor lungs (n = 28) served as a control. Patient and donor characteristics are summarized in Table 1.

2.2. Animal experiments

All animal experiments were performed in accordance with institutional and national guidelines for the care and use of experimental animals. For hypoxic exposures, male wild-type mice were placed in a ventilated chamber system with a FiO_2 of 0.10. To induce PH in rats, male Sprague-Dawley rats were injected with monocrotaline (MCT) as described previously [11]. After 21 days, MCT-injected rats and mice-exposed to hypoxia were sacrificed and lung tissue samples were prepared for further analysis. A detailed protocol of the treatment of the hypoxic mice with STI571 (Imatinib/Gleevec®, Novartis) is provided in [11].

Table 1
IPAH patient and donor characteristics for lung tissue samples.

	IPAH (n = 24)	Donor (n = 28)
Age (mean ± SD)	41.7 ± 10,8	43.9 ± 8.5
Sex (female/male; %)	72/28	67/33
mPAP (mmHg)	51.9 ± 18.8	–
NYHA classification	III–IV	–

IPAH, idiopathic pulmonary arterial hypertension; mPAP, mean pulmonary artery pressure; NYHA; New York Heart Association.

2.3. Isolation and culture of PASMC

Pulmonary artery smooth muscle cells (PASMC) used for all the experiments described in the manuscript were isolated from non-utilized human donor lungs (lungs harvested for lung transplantation that were not implanted due to lack of compatibility) or from IPAH patients lungs. The cells were isolated from human pulmonary arteries (from the third intrapulmonary branch, diameter < 1 mm). PASMC were cultured in Vasculife SMC Medium Complete Kit (Lifeline Cell Technology, Oceanside, CA) supplemented with 10 mM L-Glutamine, 5% fetal bovine serum (FBS), 5 ng/mL recombinant human (rh) epidermal growth factor, 5 μg/mL rh insulin, 50 μg/mL ascorbic acid, 5 ng/mL rh fibroblast growth factor-b (all from Lifeline Cell Technology) and 1% Penicillin/Streptomycin (Invitrogen Life Technologies, Carlsbad, CA). The cells were cultured at 37 °C in a humidified incubator with 5% CO_2.

2.4. siRNA transfection and treatment of PASMC

PASMC were transfected with siRNA at 60–70% confluence using Lipofectamine® 2000 (Thermo Fisher Scientific, Darmstadt, Germany) and analyzed 48 h thereafter. siRNA directed against human LRP1 (sense strand 5′-CCUGUAACCUGCAGUGCUUdTdT-3′) was synthesized by Microsynth AG (Lindau, Germany) and the control siRNA was purchased from Ambion (Austin, TX). In some experiments, PASMC were treated with the following reagents: 12.5 μg/mL cycloheximide (Sigma-Aldrich, Hamburg, Germany), 10 ng/mL PDGF-BB (R&D Systems, Wiesbaden, Germany), 2 μM Imatinib (Sigma-Aldrich), 10 μg/mL anti-PDGF-BB neutralizing antibody (R&D Systems), 10 μg/mL β1 integrin-blocking antibody (clone P5D2; Abcam, Berlin, Germany), 10 μg/mL β4 integrin-blocking antibody (clone ASC-3; Millipore, Darmstadt, Germany), or 10 μg/mL respective isotype control antibody (BD Bioscience, Franklin Lakes, NJ).

2.5. Protein isolation and western blotting

Proteins were isolated in a lysis buffer containing 50 mM Tris, pH 7.4, 150 mM NaCl, 1 mM EDTA, 1% Triton-X-100, 1% Sodium Deoxycholate and 0.1% SDS supplemented with 1 mM Na_3VO_4, 1 mM PMSF and 1 μg/mL Complete Protease Inhibitor Cocktail (Roche Applied Science, Indianapolis, IN), separated on a 10% SDS polyacrylamide gel and transferred to a PVDF membrane (Roth, Karlsruhe, Germany). The membrane was blocked with 1% bovine serum albumin (BSA) and treated with one of the following antibodies: rabbit anti-LRP1 (Abcam), rabbit anti-α5-integrin (Cell Signaling Technology, Leiden, The Netherlands), mouse anti-α-smooth muscle actin (α-SMA; Thermo Fisher Scientific), mouse anti-myocardin (R&D Systems, Wiesbaden, Germany), mouse anti-fibronectin (FN; Enzo Life Science, Loerrach, Germany), goat anti-collagen I (SouthernBiotech, Birmingham, AL), mouse anti-osteopontin (OPN; Santa Cruz Biotechnology, Santa Cruz, CA) and mouse anti-β1-integrin (BD Biosciences). Proteins were detected using either Amersham ECL Select Western Blotting Detection Reagent (GE Healthcare, Chicago, IL) or Pierce ECL Western Blotting Substrate (Thermo Fisher Scientific). The pictures were acquired using a ChemiDoc Imaging Systems (Bio-Rad, Hercules, CA). α-Tubulin, detected using a rabbit-anti α-tubulin antibody (Cell Signaling), was used as a loading control. Protein extraction from microdissected formalin-fixed and paraffin-embedded tissue was performed as previously described [12].

2.6. RNA isolation and real-time PCR

RNA isolation, reverse transcription (RT) and real-time PCR (qPCR)

were conducted as described previously [13]. The following primers were used: human *LRP1* forward: 5′-TCTACTTTGCCG-ACACCACC-3′ and reverse: 5′-TGTCTTTTTGGGCCCATCGT-3′; human β1-integrin forward: 5′-CCGCGCGGAAAAGATGAA-3′ and reverse: 5′-CACAATTTG GCCCTGCTTGTA-3′; human *α-SMA* forward: 5′-GTGTTGCCCCTGAAG AGCAT-3′ and reverse: 5′-CGCCTGGATAGCCACATACAT-3′; human myocardin forward: 5′-AGGTAACACAGCCTCCATCCT-3′ and reverse: 5′-TCTAGCGTCTGCTGGCATTT-3′; human *FN* forward: 5′-CACCTCTG TGCAGACCACATC-3′ and reverse: 5′-GTCTCTTGGCAGCTGACTCCG-3′; human *OPN* forward: 5′-GAAGATGATGATGACCATGTG-3′ and reverse: 5′-GTCAGGTCTGCGAAACTTC-3′ human *PBGD* (porphobilinogen deaminase) forward: 5′-ACCCTAGAAACCCTGCCAGAGAA-3′ and reverse: 5′-GCCGGGTGTTGAGGTTTCCCC-3′; rat *Lrp1* forward: 5′-CGTCACTTA CATCAACAACC-3′ and reverse: 5′-CAGCCATTCACATTTCTTGC-3′; rat *Pbgd* forward: 5′-GCCAGAGAAAAGTGCCG-TGGGG-3′ and reverse: 5′-CCAGCTTCCGTAGGCGGGTG-3′; murine *Lrp1* forward: 5′-CGCCTGT GAGAATGACCAGT-3′ and reverse: 5′-TCTAATGATGCCTGGGC-3′ and murine *Pbgd* forward: 5′-GCCAGAGAAAAGTGCCGTGGG-3′ and reverse: 5′-TCCGGAGGCGGGTGTTGAGG-3′. Changes in gene expression are reported as a ΔCt ($Ct_{PBGD} - Ct_{Gen\text{-}of\text{-}interest\ (GOI)}$). Values calculated in this way are proportional to the −log normalized amount of the GOI. In order to check for exclusive amplification of a PCR product, melting-curve analysis and gel electrophoresis were performed. Alternatively, gene expression was analyzed using the Extracellular Matrix and Adhesion Molecules RT^2 Profiler PCR Array (Qiagen, Hilden, Germany) according to the manufacturer's instructions. Changes in RNA expression of each target gene were normalized using averages of Ct values of the following reference genes (β-actin, β_2-microglobulin, glyceraldehyde-3-phosphate dehydrogenase, and hypoxanthine phosphoribosyltransferase). Changes in a target gene expression are reported as ΔΔCt ($Ct_{average\ of\ reference\ genes} - Ct_{GOI})_{siLRP1} - (Ct_{average\ of\ reference\ genes} - Ct_{GOI})_{siCtrl}$ from 3 biological replicates.

2.7. Analysis of microRNA103/107 expression

Total RNA was isolated from PASMC using the TRIZOL reagent according to the manufacturer's instruction (Invitrogen Life Technologies). After DNase I treatment, 1 μg RNA was reverse transcribed in the reaction containing 50 nM stem-loop RT primer each (microRNA103: 5′-GTCGTATCCAGTGCAGGGTCCGAGGTATTCGCACT GGATACGACT-CATAG-3′ and microRNA107: 5′-GTCGTATCCAGTGCA GGGTCCGAGGTATTCGCACTG-GATACGACTGATAG-3′), 2 μL 1× RT buffer, 4 mM dNTP mix, 2.5 U/μL MultiScribe Reverse Transcriptase, 1 U/μL RNase Inhibitor (all from Applied Biosystems, Waltham, MA) in a volume of 20 μL. The RT reaction was carried out at 16 °C for 30 min, at 42 °C for 30 min and at 85 °C for 5 min. The following controls were included: no-RNA, no stem-loop RT primer, and no reverse transcriptase. MicroRNA103/107 levels were measured using SYBR Green qPCR Master Mix (Applied Biosystems) according to the manufacturer's instruction. All primers were used in the final concentration of 200 nM and the sequences were as followed: microRNA103/107 forward: 5′-CACGCAAGCAGCATTGTA-3′ (recognizes microRNA103 and microRNA107) and reverse 5′-GTGCAGGGTCCGAGGT-3′ and ribosomal protein lateral stalk subunit P0 (*RPLP0*) forward: 5′-CCTTCTCC TTTGGGCTGGTCATCCA-3′ and reverse 5′-CAGACACTGGCAACATT GCG-GACAC-3′. The reaction mix was incubated at 95 °C for 10 min, followed by 40 cycles of 95 °C for 15 s and 60 °C for 60s. Melting curve analysis and gel electrophoresis were performed to confirm the exclusive amplification of the expected qPCR product. Changes in microRNA103/107 expression are presented as a ΔCt ($Ct_{RPLP0} - Ct_{microRNA103/107}$).

2.8. Cell surface biotinylation

Cell surface proteins were labeled with 0.5 mg/mL EZ-Link™ Sulfo-NHS-SS-Biotin (Thermo Fisher Scientific) for 1 h at 4 °C. After quenching with 100 mM glycine, protein isolation was performed as described above. Hundred microgram biotinylated proteins were incubated with Pierce™ NeutrAvidin™ Agarose beads (Thermo Fisher Scientific) overnight at 4 °C. Following extensive washing with buffers containing 50 mM TRIS, pH 7.4, 5 mM EDTA and increasing concentration of NaCl (150–500 mM), the proteins were analyzed by western blotting.

2.9. Flow cytometry

PASMC were trypsinized and fixed with 2% paraformaldehyde for 10 min at room temperature. Afterwards, the cells were washed with phosphate-buffered saline (PBS), blocked with 1% BSA for 1 h at room temperature and surface-labeled with a rat anti-β1- integrin (clone 9EG7; BD Biosciences) or an isotype control (BD Bioscience) antibody overnight at 4 °C. Subsequently, the samples were washed and incubated with a fluorescein isothiocyanate (FITC)-labeled secondary antibody (Jackson Immunoresearch, Cambridge, United Kingdom) for 2 h at 4 °C. Flow cytometry was carried out with Accuri C6 flow cytometer and the data was analyzed using CFlowPlus (BD Biosciences) software.

2.10. Cell adhesion assay

For cell adhesion analysis, 1×10^4 cells were seeded onto a 96-well-plate coated with 2 μg/mL human FN (Sigma-Aldrich). After 40 min incubation at 37 °C, the cells were fixed with cold methanol/acetone solution (1:1) for 1 h at 4 °C, dried and subsequently stained with crystal violet (Sigma-Aldrich). Afterwards, the cells were lysed using 10% acetic acid. The absorbance was measured at 560 nm with a microplate reader (SpectraMax 190, Molecular Devices, Biberach, Germany).

2.11. Transwell migration assay

Cell migration was tested using polycarbonate membrane transwell inserts (8 μm pore size, BD Biosciences) coated with 2 μg/mL human FN (Sigma-Aldrich) overnight at 4 °C. 1×10^4 of PASMC resuspended in 350 μL serum-free medium were added to the upper chamber of the transwell. Next, 350 μL of medium containing 5% FCS was applied to the bottom chamber and the cells were allowed to migrate through the membrane for 24 h. Afterwards, the cells from the upper chamber were removed using a cotton swab and the cells that migrated through the membrane were fixed with a methanol/acetone solution, stained with crystal violet and counted under the microscope.

2.12. Cell proliferation assay

PASMC proliferation was measured by ^{3}H-thymidine incorporation. Forty eight h after seeding onto a 48-well-plate (2×10^3 cells/well), 0.6 μCi/mL ^{3}H-thymidine (PerkinElmer Life Sciences, Hopkinton, MA) in growth medium supplemented with 5% FCS was applied to the cells for 20 h. Following extensive washing with PBS and cell solubilization in 0.5 M NaOH, ^{3}H-thymidine content was quantified by liquid scintillation spectrometry (Beckman LS 6500, Fullerton, CA).

2.13. Generation of Acta2-cre/ERT2; $Lrp1^{flox/flox}$ mice

Transgenic mice expressing a tamoxifen-inducible Cre recombinase under the Acta2 promoter (B6;Tg(Acta2-cre/ERT2)12Pcn [14]) were crossed with mice bearing floxed allele of *Lrp1* gene (Lrp1 < tm2Her > /J [15]. The resulting mouse strain (B6;Tg(Acta2-cre/ERT2) 12Pcn; Lrp1 < tm2Her > /J, referred to herein as Acta2-Cre^{ERT2}; $Lrp1^{flox/flox}$) was then back-crossed for eight generations to C57BL/6J background and used for the experiments. Littermates that were homozygous for the floxed *Lrp1* allele but did not carry Acta2-Cre^{ERT2}

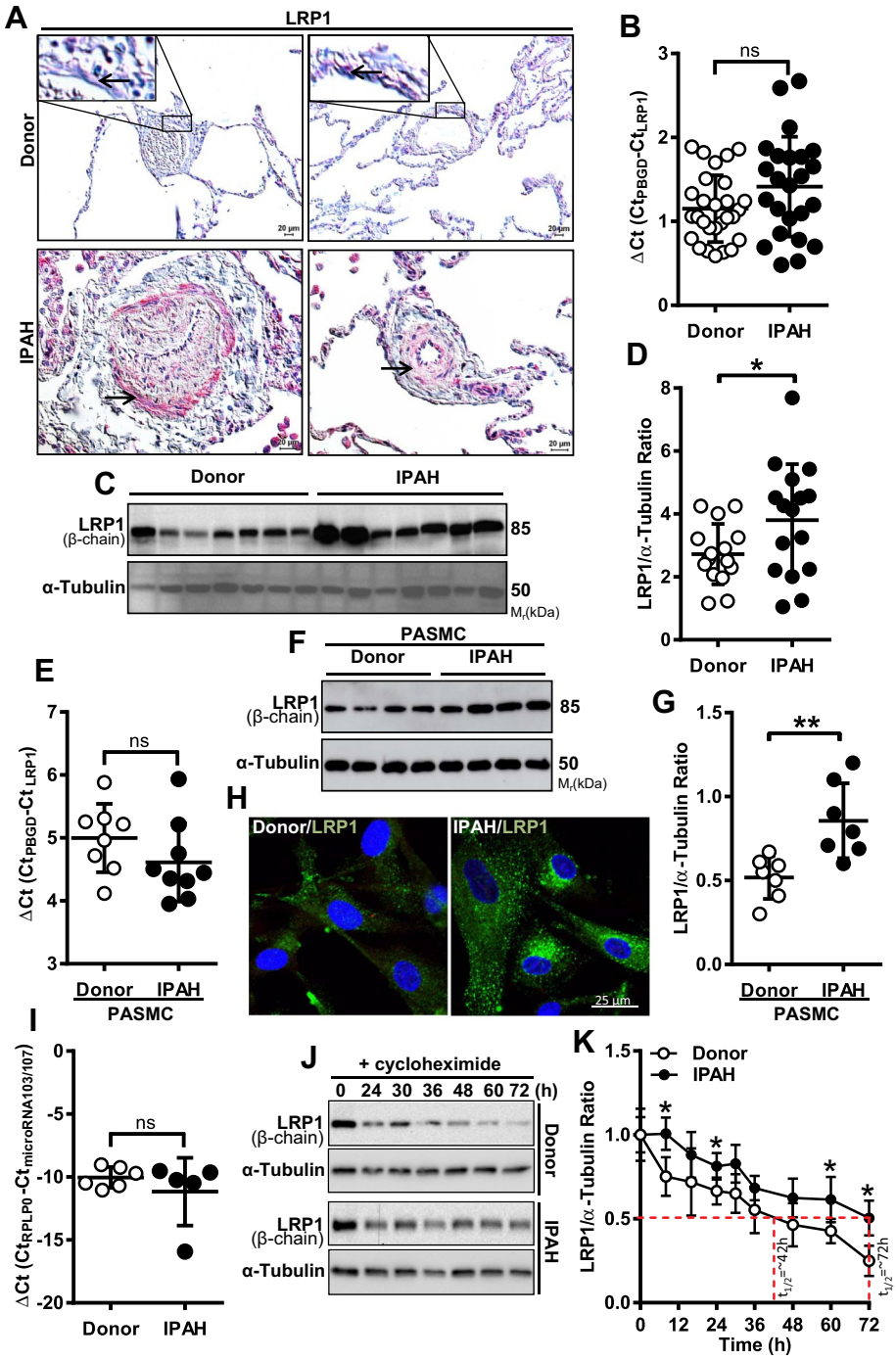

Fig. 1. LRP1 protein levels are increased in lungs and PASMC of IPAH patients. (A) Immunohistochemistry for LRP1 in lungs of donors and IPAH patients. Arrows indicate media of pulmonary vessels. Scale bar = 20 µm. (B, C) LRP1 mRNA (B) and protein levels (C) in lung homogenates of donors (n = 28 for RNA, n = 14 for protein) and IPAH patients (n = 24 for RNA, n = 16 for protein). The qPCR data are presented as ΔCt using *PBGD* as a reference gene. For western blotting, α-tubulin was used as a loading control. Representative blots are shown. (D) Densitometry analysis of (C). (E, F) LRP1 mRNA (E) and protein (F) levels in pulmonary arterial smooth muscle cells (PASMC) of donors (n = 8 for RNA, n = 7 for protein) and IPAH patients (n = 9 for RNA, n = 7 for protein). The qPCR data are expressed as ΔCt using *PBGD* as a reference gene. For western blotting, α-tubulin was used as a loading control. Representative blots are shown. (G) Densitometry analysis of (F). (H) Immunofluorescence staining for LRP1 in PASMC isolated from donor and IPAH lungs. Scale bar = 25 µm. (I) microRNA103/107 expression in donor (n = 6) and IPAH (n = 5) PASMC. The qPCR data are presented as ΔCt using *RPLP0* as a reference gene. (J) Time course of LRP1 protein stability in donor and IPAH PASMC exposed to 12.5 µg/mL cycloheximide as assessed by western blotting. α-Tubulin served as a loading control. Representative blots are shown. (K) Densitometry analysis of (J). LRP1/α-tubulin ration at time point 0 was set to 1 (n = 5). ns, not significant, *p < 0.05, **p < 0.01.

cassette (Lrp1$^{flox/flox}$) were used as controls.

2.14. Preparation of precision cut lung slices (PCLS)

PCLS were prepared from Acta2-Cre^{ERT2}; Lrp1$^{flox/flox}$ and Lrp1$^{flox/flox}$ mice sacrificed by cervical dislocation and exsanguinated by transection of the Arteria renalis. The trachea was cannulated with a Vasofix® Safety intravenous catheter and 2.5 mL of 1.5% low-melting point agarose dissolved in serum-free DMEM was injected into the lungs. After 5 min, the lungs were removed and tissue cores of a diameter of 8 mm were prepared using a sharp rotating metal tube. Subsequently, the cores were sliced into 300–350 µm thin slices in DMEM using a Krumdieck tissue slicer (Alabama Research and Development, Munford, AL). PCLS were washed 3× for 30 min in DMEM supplemented with 100 U/mL penicillin, and 100 µg/mL streptomycin (both from Biochrom, Berlin, Germany) and used for the experiments. To induce *Lrp1* gene inactivation, PCLS were treated with 5 µM 4-hydroxy tamoxifen (4-OH TXN; Cayman Chemical, Hamburg, Germany) dissolved in ethanol for 48 h. Viability of the tissue was assessed by a LDH Cytotoxicity Detection Kit (Roche, Mannheim, Germany) according to manufacturer's instruction.

2.15. Immunohistochemistry

Lung tissue specimens were fixed with 4% paraformaldehyde in PBS and embedded in paraffin. One micrometer sections were deparaffinized in xylene and rehydrated through graded ethanol washes. Antigen retrieval was achieved by cooking tissue sections in Decloaker

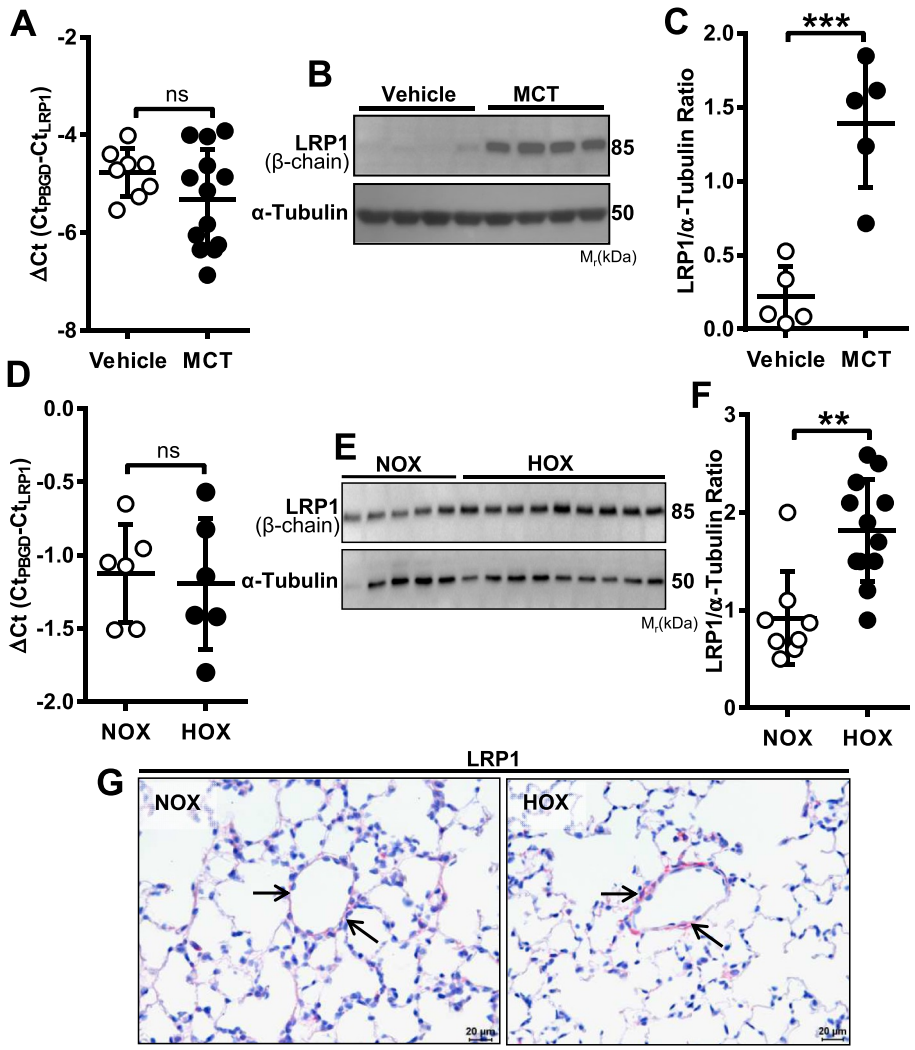

Fig. 2. LRP1 protein expression is elevated in the lungs of experimental models of PH. (A, B) LRP1 mRNA (A) and protein levels (B) in lung homogenates of rats treated either with vehicle (n = 8 for RNA, n = 5 for protein) or monocrotaline (MCT, n = 13 for RNA, n = 5 for protein). The qPCR data are expressed as ΔCt using *Pbgd* as a reference gene. For western blotting, α-tubulin was used as a loading control. Representative blots are shown. (C) Densitometry analysis of (B). (D, E) LRP1 mRNA (D) and protein levels (E) in lung homogenates of mice maintained either under normoxic (NOX) (n = 6 for RNA, n = 8 for protein) or hypoxic (HOX) (n = 6 for RNA, n = 12 for protein) conditions. The qPCR data are expressed as ΔCt using *Pbgd* as a reference gene. For western blotting, α-tubulin was used as a loading control. Representative blots are shown. (F) Densitometry analysis of (E). (G) Immunohistochemistry for LRP1 in lungs of NOX and HOX mice. Arrows indicate pulmonary vessels. Scale bar = 20 µm. ns, not significant, **p < 0.01, ***p < 0.001.

Reagent (Zymed Laboratories Inc., San Francisco, CA) for 20 min. After cooling, tissue sections were blocked with 10% BSA in PBS for 1 h and then incubated overnight at 4 °C with one of the following antibodies: rabbit anti-LRP1 (Abcam), rabbit anti-PCNA (Cell Signaling Technology) and rabbit anti-α-SMA (Sigma-Aldrich). Antigen detection was performed using a ZytoChem-Plus AP Polymer-Kit in accordance with the manufacturer's instruction (Zymed Laboratories Inc.).

2.16. Immunofluorescence staining

PASMC from donor or IPAH lung tissue were seeded in a 8-well chamber slide (2×10^4/well) and cultured for 48 h. The cells were washed with PBS, fixed with ice-cold methanol for 20 min at −20 °C, permeabilized with 0.02% TritonX for 10 min, and blocked with 3% BSA in PBS for 1 h. Afterwards, PASMC were incubated overnight at 4 °C with mouse anti-LRP1 antibody (Abcam). After washing 3× with PBS, the cells were incubated with AlexaFluor 488-labeled anti-rabbit secondary antibody (Invitrogen) for 1 h at room temperature. Finally, the slides were mounted with DAPI mounting medium (Vectashield, Vector Labs, Burlingame, CA). Images were taken using a laser scanning confocal microscope (Nikon A1R Ultra-Fast Spectral Scanning Confocal Microscope; Tokyo, Japan) with CFI Plan Apochromat Lambda 60×/1.4 oil immersion objective.

2.17. Statistical analysis

Student's *t*-test was used for the comparison between two groups. Analysis of variance followed by Tukey's *post hoc* test was applied for the comparison of multiple groups. $p < 0.05$ was considered statistically significant. Data are expressed as mean ± SD of at least three independent experiments.

3. Results

3.1. LRP1 levels in lungs and cells from IPAH patients

To assess the role of LRP1 in PH, we first analyzed the distribution and expression of this receptor in human lung tissue samples. In the lungs of patients suffering from idiopathic pulmonary artery hypertension (IPAH), strong LRP1 immunoreactivity was observed in SMC and EC of the remodeled pulmonary vessels (Fig. 1A). In donor lungs, the pulmonary vessel wall was only weakly stained for LRP1 (Fig. 1A). On the mRNA level there was no difference in the *LRP1* expression between lung tissue samples obtained from donors and IPAH patients (Fig. 1B), however, on the protein level marked upregulation of LRP1 expression in diseased lungs was noted (Fig. 1C and D). Similarly, *LRP1* mRNA levels were not changed in PASMC isolated from IPAH lungs as compared to PASMC obtained from donor lungs (Fig. 1E), but LRP1 protein was significantly increased in IPAH PASMC as opposed to donor PASMC (Fig. 1F and G). Immunocytochemistry conducted on PASMC

isolated from donor and IPAH lungs confirmed this finding (Fig. 1H). As LRP1 protein levels in SMC were found to be regulated by microRNA103/107 [16], we next evaluated the expression of these microRNAs in PASMC isolated from donor and IPAH lungs. However, no difference in the expression of microRNA103/107 between two experimental groups was measured (Fig. 1I). To further explore this, we incubated cells with cycloheximide, an inhibitor of protein synthesis. As depicted in Fig. 1J and K half-life of LRP1 in donor PASMC was about 42 h whereas in IPAH PASMC was about 72 h. This suggests that the increased LRP1 protein stability may account for the high LRP1 protein abundance in IPAH.

3.2. LRP1 levels in lungs of rats treated with monocrotaline and mice exposed to hypoxia

Next, we analyzed the expression of LRP1 in lung tissue samples obtained from experimental models of PH, rats challenged with monocrotaline (MCT) and mice maintained under hypoxic conditions (HOX). Although, *Lrp1* mRNA levels were not altered in MCT-injected rats, on the protein level strong elevation of the LRP1 expression in this experimental group was observed (Fig. 2A–C). In mouse exposed to hypoxia, LRP1 protein (Fig. 2E and F), but not *Lrp1* mRNA (Fig. 2D), was significantly increased. Furthermore, LRP1 staining was more intense in pulmonary vessels of HOX mice as compared to animals maintained under normoxic (NOX) conditions (Fig. 2G). Unfortunately, none of the antibodies tested was suitable for LRP1 immunostaining in rat lung tissue.

3.3. Regulation of LRP1 expression in PASMC

As PDGF-BB is one of the main mediators of PH [17], we next investigated whether this growth factor may influence LRP1 expression in isolated PASMC. Treatment of PASMC with PDGF-BB did not elevate *LRP1* mRNA levels (Fig. 3A). On the protein level, however, a time-dependent increase in the LRP1 expression following exposure of PASMC to PDGF-BB was observed (Fig. 3B and C). PDGF-BB-induced LRP1 protein expression was attenuated by PDGF-BB neutralizing antibody or the PDGF receptor antagonist Imatinib (Fig. 3D and E). Imatinib also attenuated LRP1 synthesis in lung tissue of mice maintained under HOX conditions (Fig. 3F and G). In addition, LRP1 immunoreactivity was reduced in the pulmonary vessels of HOX mice treated with Imatinib, as compared to controls (Fig. 3H).

3.4. LRP1 controls PASMC activities

We then analyzed the impact of LRP1 depletion on PASMC proliferation, adhesion, and migration. LRP1 knock-down efficiency is shown in Fig. 4A and B. LRP1 silencing significantly reduced proliferation of PASMC (Fig. 4C). On the contrary, migration and adhesion were increased in LRP1 depleted PASMC (Fig. 4D–F). In addition, we investigated the expression of proteins involved in the PASMC phenotypic switch from a differentiated (contractile) to a de-differentiated (synthetic) state. The markers of the contractile phenotype are, among others, α-smooth muscle actin (α-SMA) and myocardin (Myoc), whereas the synthetic phenotype is generally characterized by a high expression of ECM components including collagen I (Col I), fibronectin (FN), and osteopontin (OPN) [4,18]. On the mRNA level, the elevation of the *Myoc* expression following LRP1 silencing was observed (Fig. 4G). On the protein level, the changes in the expression of Myoc were accompanied by elevated α-SMA and lower Col I and FN synthesis (Fig. 4H and I). Altogether, these results suggest that low LRP1 levels may support differentiated PASMC phenotype.

3.5. LRP1 regulates proliferation of SMC in 3D ex vivo murine lung tissue cultures

To demonstrate that LRP1 controls proliferation of PASMC in more complex biological systems, we knocked-out the *Lrp1* gene in precision cut lung slices (PCLS) prepared from Acta2-Cre^{ERT2}; Lrp1$^{flox/flox}$ mice. As depicted in Fig. 5A–C the induction of Cre recombinase activity with 4-hydroxy tamoxifen (4-OH TXN) treatment allowed selective and efficient LRP1 depletion in SMC. Exposure of PCLS generated from Lrp1$^{flox/flox}$ mice to 4-OH TXN excluded the impact of 4-OH TXN on LRP1 expression in pulmonary vessels (Fig. 5B and C). Trace amounts of LRP1in 4-OH TXN-treated PCLS derived from Acta2-Cre^{ERT2}; Lrp1$^{flox/flox}$ mice may originate from EC of microdissected pulmonary vessels (Fig. 5B and C). Furthermore, 4-OH TXN-induced genetic ablation of *Lrp1* in Acta2-Cre^{ERT2}; Lrp1$^{flox/flox}$ PCLS increased α-SMA expression in pulmonary vessels (Fig. 5B and C) and lowered the number of PCNA-positive cells in pulmonary vasculature (Fig. 5D and E).

3.6. LRP1 affects cell proliferation via regulation of β1-integrin expression

As cell-ECM interactions are crucial for cell growth and (de)-differentiation, we next investigated the expression of molecules involved in cell-ECM communication in LRP1-depleted PASMC. LRP1 silencing upregulated mRNA levels of tenascin C (*TNC*), tissue inhibitor of metalloproteinase (*TIMP*) 3, *MMP8*, collagen XV (*COL15A1*), thrombospondin 2 (*THBS2*), β4-integrin (*ITGB4*) and *MMP11*. The gene expression levels of *MMP14*, *MMP13*, *MMP15*, α1-integrin (*ITGA1*), collagen XI (*COL11A1*), β1-integrin *(ITGB1)* and intercellular adhesion molecule 1 (*ICAM1*) mRNA were downregulated following LRP1 knockdown (Fig. 6A). Integrins are transmembrane receptors that integrate cues from ECM with intracellular signaling machinery, thus regulating multiple cell functions including proliferation [19]. Hence, we decided to further investigate the role of integrins in LRP1-triggered changes in PASMC growth. To this end, we first validated alterations in protein expression of β1-integrin subunit in PASMC following LRP1 knockdown. As depicted in Fig. 6B and C, silencing of LRP1 reduced the expression of the mature (125 kDa band) and immature (100 kDa band) form of β1-integrin and lowered the abundance of α5-integrin (β1-integrin interaction partner). Likewise, downregulation of β1- and α5-integrin expressions were observed in the cytosolic and membrane fraction of LRP1 depleted PASMC (Fig. 6D). Concomitantly, the levels of active β1-integrin on the cell surface of PASMC transfected with LRP1-targetting siRNA were diminished (Fig. 6E).

Since reduced proliferation of LRP1-depleted PASMC was accompanied by decreased β1-integrin levels, we hypothesized that LRP1 may stimulate PASMC proliferation by supporting β1-integrin expression. A β1-integrin function-blocking antibody reduced proliferation of LRP1-expressing PASMC to the level observed in the control cells transfected with LRP1-targetting siRNA (Fig. 6F). Simultaneous LRP1 depletion and β1-integrin blockage did not further potentiated a growth-inhibitory effect suggesting that LRP1 regulates PASMC proliferation in a β1-integrin-dependent manner (Fig. 6F). As LRP1 knockdown altered the expression of β4-integrin, we also tested the functional impact of the increased β4-integrin levels in LRP1-depleted PASMC. As seen in Fig. 6F, a β4-integrin function-blocking antibody did not restore cell proliferation following LRP1 silencing.

3.7. LRP1 controls activities of IPAH PASMC

Next, we examined whether IPAH PASMC, which exhibit high LRP1 levels, demonstrate elevated expression of β1-integrin. Indeed, PASMC isolated from IPAH patients displayed significantly increased β1-integrin expression when compared to the cells isolated from donor lungs (Fig. 7A–C). Furthermore, silencing of LRP1 strongly diminished β1 integrin levels in IPAH PASMC, thus, suggesting a pivotal role of LRP1 in the regulation of β1-integrin expression under physiological and

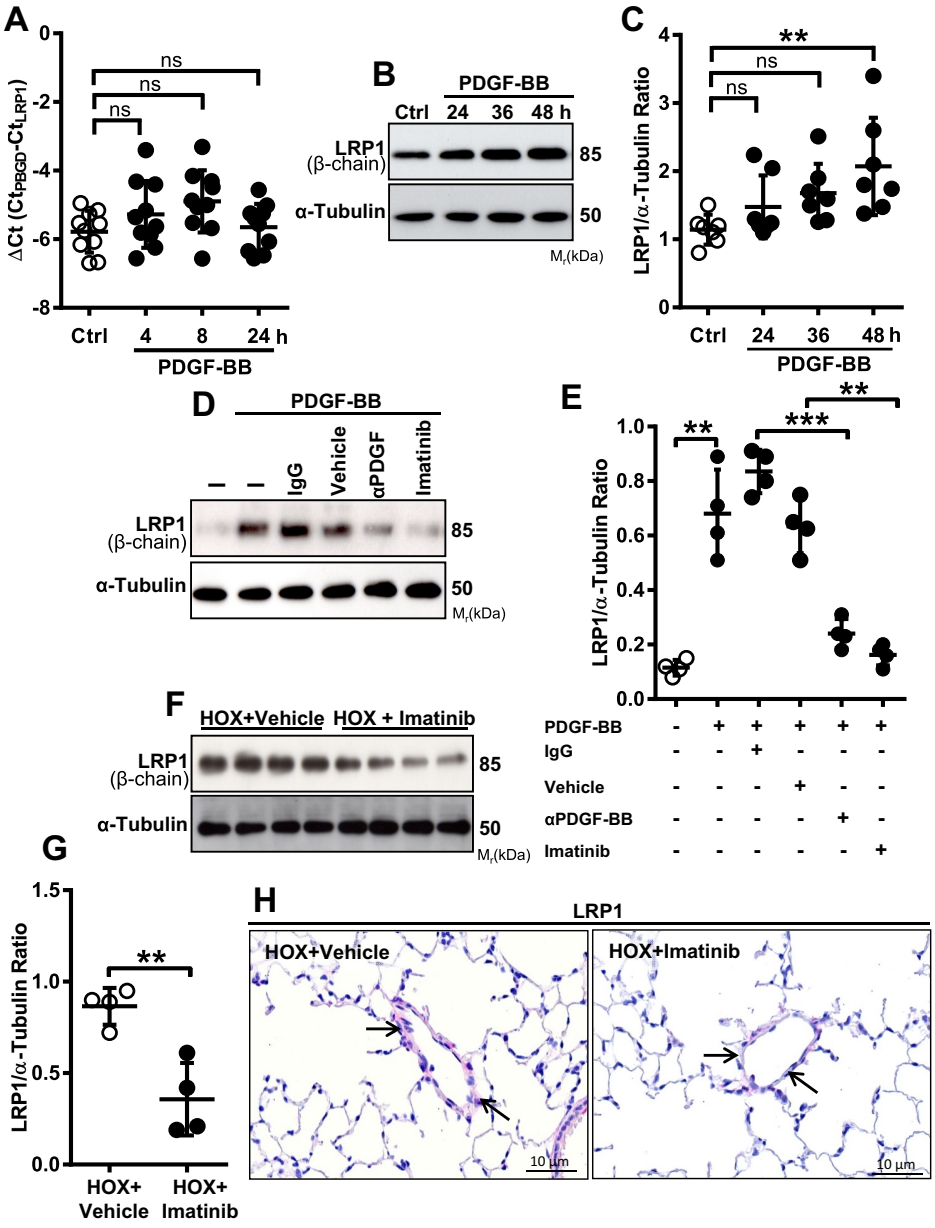

Fig. 3. PDGF-BB potentiates LRP1 protein expression in PASMC and lungs of mice exposed to hypoxia. (A, B) LRP1 mRNA (A) and protein levels (B) in donor PASMC treated with 10 ng/mL of PDGF-BB for indicated time points. The qPCR data are expressed as ΔCt using *PBGD* as a reference gene (n = 10). Protein levels were assessed by western blotting using α-tubulin as a loading control. Representative blots are shown. (C) Densitometry analysis of (B) (n = 7). (D) LRP1 protein levels in donor PASMC treated with 10 ng/mL of PDGF-BB in the absence or presence of 10 μg/mL of anti-PDGF-BB neutralizing antibody or 2 μM Imatinib. IgG antibody and vehicle were used as controls. For western blotting, α-tubulin served as a loading control. Representative blots are shown. (E) Densitometry analysis of (D) (n = 4). (F) LRP1 protein levels in lung homogenates of mice maintained under hypoxic (HOX) conditions and treated with either vehicle or Imatinib. For western blotting, α-tubulin served as a loading control. (G) Densitometry analysis of (F); n = 4/group. (H) Immunohistochemistry for LRP1 in lungs of HOX mice treated with either vehicle or Imatinib. Scale bar = 10 μm. ns, not significant, **p < 0.01, ***p < 0.001.

pathological conditions (Fig. 7D and E). Blockage of β1-integrin reduced proliferation of IPAH PASMC to the level observed in control donor cells (Fig. 7F) and simultaneous LRP1 depletion and β1-integrin inhibition did not augment the growth-inhibitory effect when compared to IPAH PASMC treated with siLRP1 or the β1-integrin function-blocking antibody alone (Fig. 7G). Finally, we tested whether depletion of LRP1 in PASMC isolated from IPAH lungs may restore their differentiated phenotype. Whereas on the mRNA level the reduction in the expression of *OPN* following LRP1 silencing was observed (Fig. 7H), on the protein level only downregulation of Col I expression in LRP1 depleted samples was apparent (Fig. 7I and J).

4. Discussion

Previous reports highlighted the role of LRP1 in several vascular pathologies, particularly in atherosclerosis and aortic aneurysms. [8,20–22]. Here, we show for the first time the increased LRP1 protein expression in the lung tissue and PASMC isolated from IPAH patients. Furthermore, we report increased LRP1 protein levels in the lungs from two animal models of PH: in rats treated with monocrotaline and in mice subjected to hypoxia. Differential regulation of other members of the LDL receptor family has already been observed in the context of PH. An increased expression of low-density lipoprotein receptor with 11 binding repeats (LR11) has been demonstrated in hypoxia-exposed mice and *Lr11* gene inactivation reduced right ventricular systolic pressure, right ventricular hypertrophy, and medial thickening in pulmonary arteries [23]. Mechanistically, LR11 and its soluble form (sLR11) were shown to mediate pathological vascular remodeling by stimulating PASMC proliferation in response to hypoxia and PDGF-BB. Interestingly, increased serum levels of sLR11 positively correlated with pulmonary vascular resistance and mean pulmonary arterial pressure in patients with PH [23]. Together with our findings of a pro-proliferative function of LRP1 in PASMC, these data indicate that dysregulated expression of LDL receptor family members contributes to the medial thickening of pulmonary arteries and thus to the pathogenesis of PH. This is in contrast to the role of LRP1 in systemic circulation, where LRP1 was reported to be crucial for maintaining SMC contractile function and vessel wall integrity [24]. These distinct functions of LRP1 in SMC of a different origin may be explained by diverse sensing mechanisms and thus by the reactions of the pulmonary and systemic

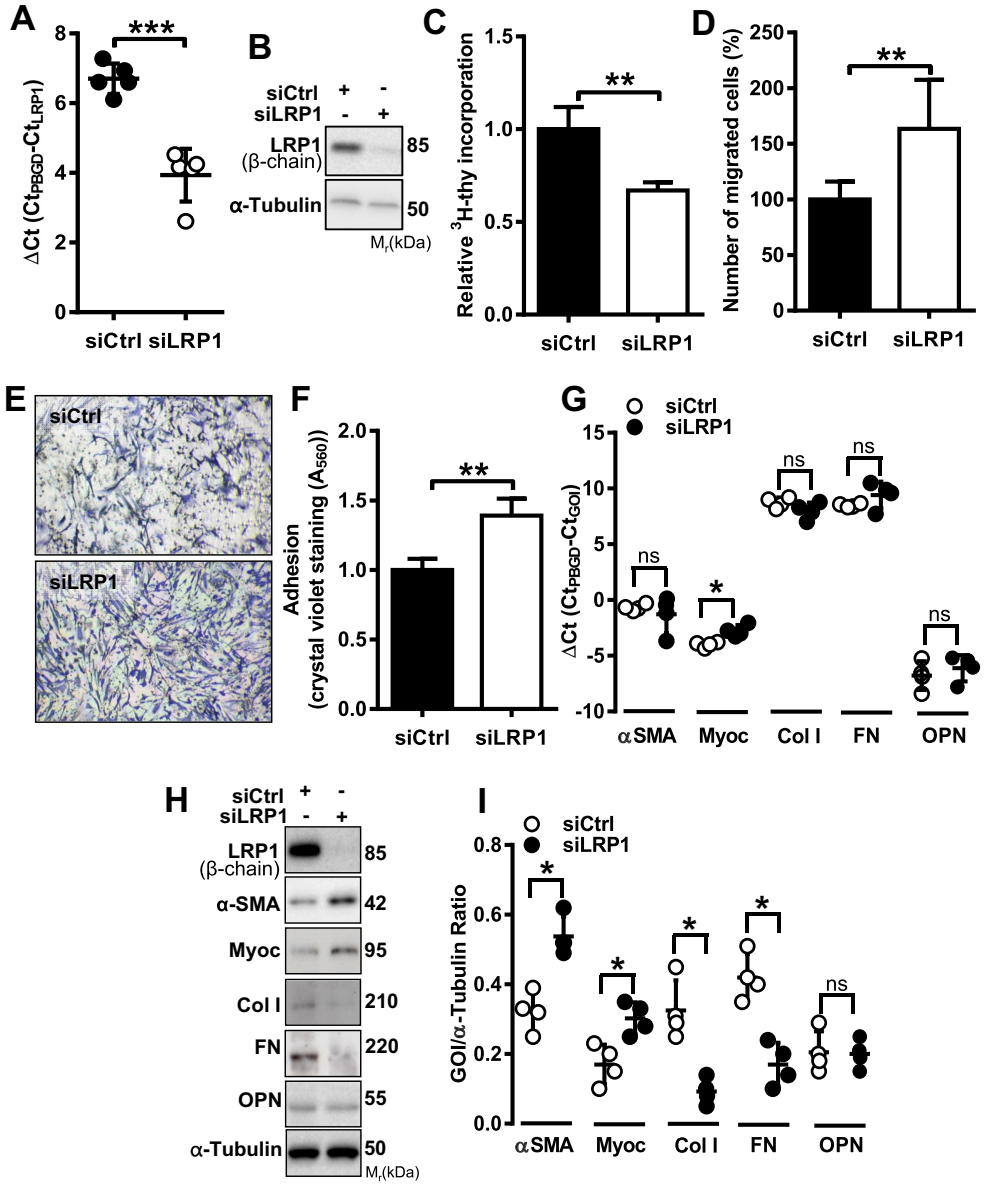

Fig. 4. LRP1 regulates PASMC activities. (A, B) Efficacy of LRP1 knockdown in donor PASMC as assessed by qPCR (A) and by western blotting (B). The qPCR data are expressed as ΔCt using *PBGD* as a reference gene (n = 5). Protein levels were assessed by western blotting using α-tubulin as a loading control. Representative blots are shown (n = 5). (C) Proliferation of donor PASMC treated with either control siRNA (siCtrl) or with siRNA directed against LRP1 (siLRP1) as assessed by ^{3}H-thymidine incorporation (n = 4). (D, E) Migration of donor PASMC treated with either siCtrl or siLRP1 as assessed by transwell assay. Values were normalized to siCtrl treated cells, set to 100% (n = 4). Representative images of cells that have migrated through the filter are shown. (F) Adhesion of donor PASMC treated with either siCtrl or siLRP1 to fibronectin (FN) as measured by crystal violet staining (n = 4). (G, H) mRNA (G) and protein (H) levels of α-smooth muscle actin (α-SMA), myocardin (Myoc), collagen I (Col I), FN, and osteopontin (OPN) in donor PASMC treated with either siCtrl or siLRP1. qPCR results are expressed as ΔCt using *PBGD* as a reference gene (n = 4). Protein levels were assessed by western blotting using α-tubulin as a loading control. (I) Densitometry analysis of (H) (n = 4). ns, not significant, *p < 0.05, **p < 0.01, ***p < 0.001.

circulation to the environmental factors. For example, the pulmonary arteries constrict in response to hypoxia whereas systemic circulation dilates thus attempting to increase the perfusion of blood to the oxygen-deprived tissues. Given the fact that hypoxia induces LRP1 expression in SMC isolated from systemic vessels [25], it is tempting to speculate that in these cells LRP1 counteracts the vasodilatory effects of low oxygen content in blood and thus promotes vasoconstriction [24]. In pulmonary arteries, which constrict in response to hypoxia to shunt blood away from the poorly ventilated regions, hypoxia-induced LRP1 expression in PASMC (unpublished observation) promotes phenotypic changes of these cells and thus may represent a part of the physiological response that due to prolonged presence of stimuli apparently spirals out of control.

The expression of LRP1 was found to be sensitive to several factors thought to mediate the pathogenesis of PH. For example, hypoxia-inducible factor-1α (HIF1α) was reported to drive LRP1 expression in vascular SMC cultured under hypoxic conditions [26]. Furthermore, angiotensin II, a peptide hormone known to be markedly increased in the serum of progressive IPAH patients [27], was described to induce the transcription of the *LRP1* gene in the same cell type [28]. Here, we show that PDGF-BB induces LRP1 expression in PASMC *in vitro* and *in vivo*. Thus over-activation of the PDGF signaling in PH could be at least in part responsible for elevated LRP1 expression under this pathological condition. Interestingly, none of the conditions tested resulted in changes in *LRP1* transcript abundance indicating that LRP1 is predominantly regulated on the protein level in PH. Several mechanisms were found to modulate LRP1 protein synthesis and stability. Leslie et al. [29] reported the suppression of LRP1 translation by p53-mediated increased expression of miRNA-103/107 in colon cancer cells and Cal et al. [30] showed the stabilization of the LRP1 protein through downregulation of CHFR, a RING type E3 ubiquitin ligase, in vascular SMC exposed to aggregated LDL. Our results demonstrate that the increased LRP1 protein stability, but not the enhanced LRP1 protein translation, may account for the high LRP1 protein abundance in PH. Whether other factors/mechanisms, such as the *lrp1* natural antisense transcript [31], additionally contribute to the high LRP1 levels in PH needs further investigation.

Next, we tested whether LRP1 regulates PASMC proliferation, migration, and adhesion. Silencing of LRP1 reduced proliferation but potentiated migration and adhesion to fibronectin of PASMC. Given the marked upregulation of LRP1 protein expression following the exposure of PASMC to PDGF-BB, one may speculate that LRP1 propagates pro-

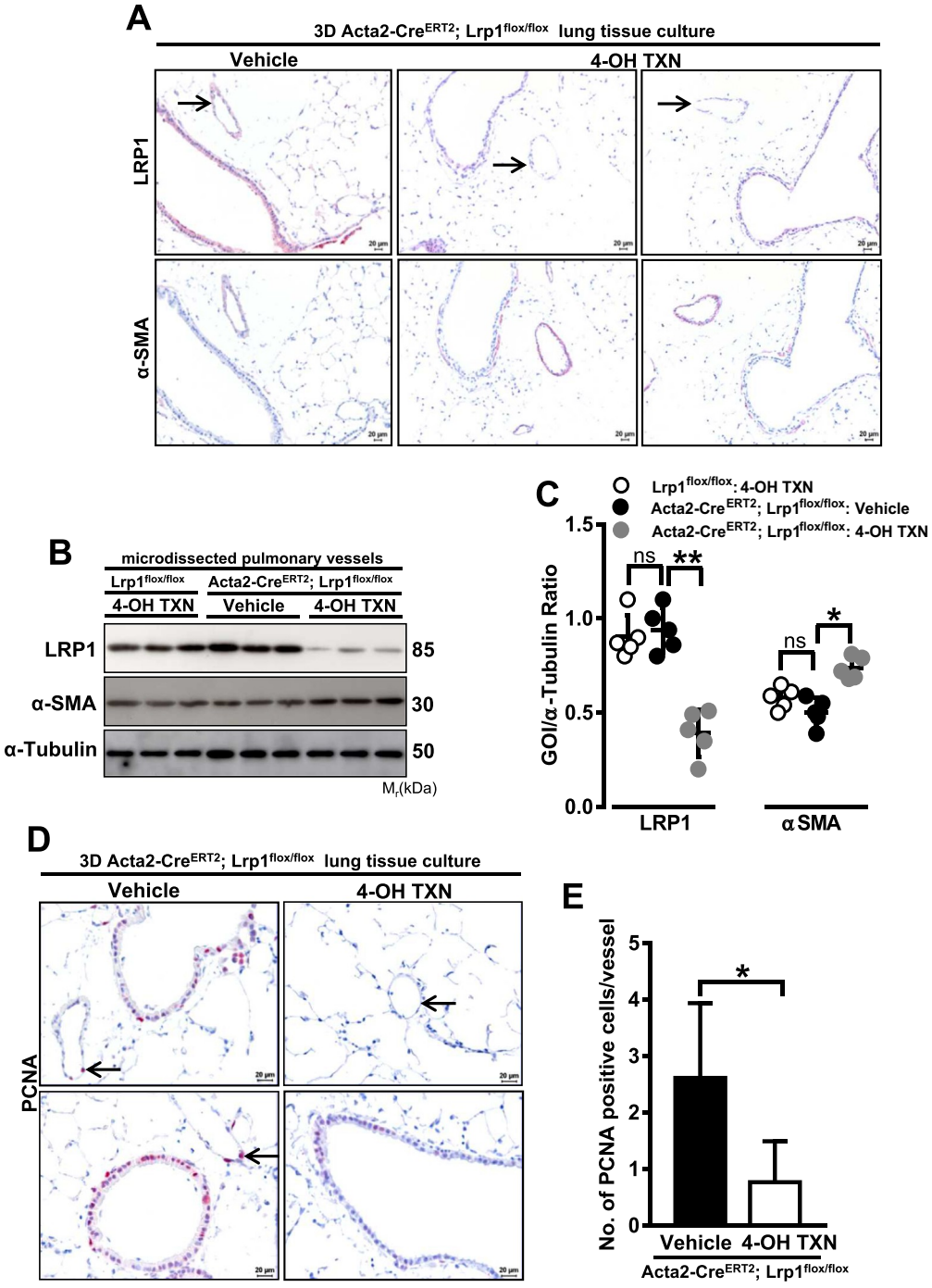

Fig. 5. SMC-specific depletion of LRP1 in 3D lung tissue cultures suppresses PASMC proliferation. (A) Immunoreactivity for LRP1 (upper panel) and α-smooth muscle actin (α-SMA, (lower panel)) in 3D *ex vivo* Acta2-Cre^{ERT2}; Lrp1$^{flox/flox}$ lung tissue cultures following treatment with vehicle or 4-hydroxy tamoxifen (4-OH TXN). Arrows indicated LRP1-positive and LRP1-negative vessel in vehicle- and 4-OH TXN-treated samples, respectively. Scale bar = 20 μm. (B) LRP1 and α-SMA protein expression in vessels microdissected from 3D *ex vivo* Lrp1$^{flox/flox}$ or Acta2-Cre^{ERT2}; Lrp1$^{flox/flox}$ lung tissue cultures following treatment with vehicle or 4-OH TXN. α-Tubulin served as a loading control in western blotting. Three biological replicates are demonstrated. (C) Densitometry analysis of (B) (n = 5). (D) Proliferating cell nuclear antigen (PCNA)-immunostaining in 3D *ex vivo* Acta2-Cre^{ERT2}; Lrp1$^{flox/flox}$ lung tissue cultures following treatment with vehicle or 4-OH TXN. Arrows indicate PCNA positive cells in pulmonary vessels. Scale bar = 20 μm. (E) Quantification of PCNA-positive cells in 20 pulmonary vessels (20–70 μm diameter) of 4 biological replicates in 3D *ex vivo* Acta2-Cre^{ERT2}; Lrp1$^{flox/flox}$ lung tissue cultures following treatment with vehicle or 4-OH TXN. ns, not significant, *p < 0.05, **p < 0.01.

proliferative effects of over-activated PDGF signaling in PH [17,32]. A complex interplay between LRP1 and the elements of PDGF signaling is thought to control vessel wall homeostasis. On the one hand, LRP1 was found to suppress PDGFRβ phosphorylation and activation of downstream signaling molecules thus repressing migration and proliferation of vascular SMC [6,20]. On the other hand, an activation of PDGF signaling was reported to induce the formation of the LRP1-PDGFRβ complex and subsequent LRP1 phosphorylation at Tyr63 within a docking site for a number of adaptor/signaling proteins, among others those involved in the propagation of cell pro-mitogenic activities [33,34]. Interestingly, PH is characterized not only by increased growth but also motility of PASMC in response to PDGF receptor ligands [17]. Thus, considering the increased LRP1 protein levels in PASMC exposed to PDGF-BB and its inhibitory role in PDGF-BB-induced SMC migration, LRP1 could eventually limit cell motility in a negative feedback loop manner. Taken together, by demonstrating the role of PDGF signaling in the regulation of LRP1 expression, our study reveals novel possibilities of bidirectional communication between these two pathways in vascular SMC.

Our PCR array analysis of LRP1 depleted PASMC revealed a differential regulation of a number of genes involved in PH. For example, LRP1 suppressed the production of *THBS2* which was shown to be down-regulated in the lungs of rats subjected to hypoxia [35]. Conversely, LRP1 supported the expression of *MMP13* and MMP14, both reported to be present at increased levels in peripheral pulmonary arteries of hypoxia-induced PH in rats [36] and in PASMC derived from IPAH lungs [37], respectively. Thus far, several studies have implicated the dysregulated expression and activity of MMPs in PH pathogenesis

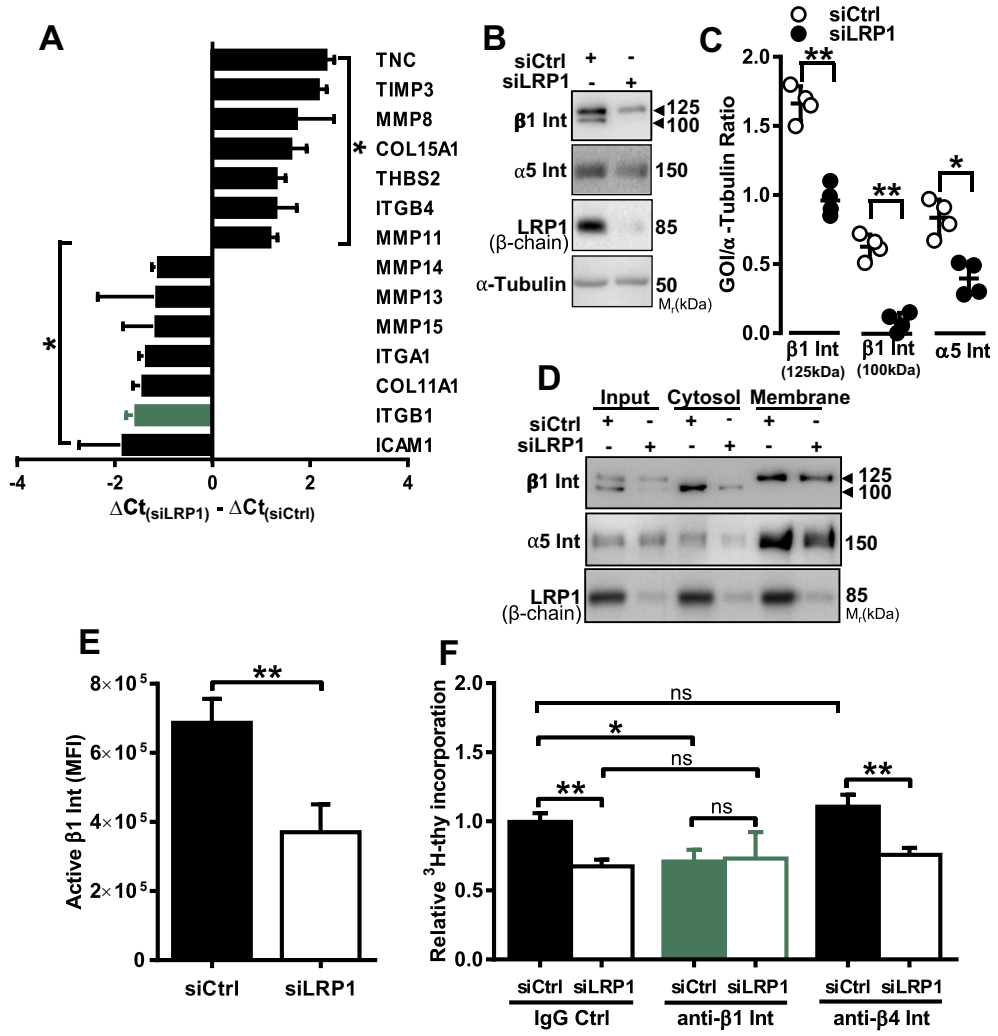

Fig. 6. LRP1 contributes to the transition of donor PASMC from the contractile to the synthetic phenotype. (A) Genes on extracellular matrix & adhesion molecules RT^2 profiler PCR array whose expression was up- or down-regulated in donor PASMC by treatment with siRNA directed against LRP1 (siLRP1). The genes listed are those where a statistically significant change ($p \leq 0.05$) in relative mRNA levels between siRNA control (siCtrl)- and siLRP1-treated cell were noted (n = 3). (B) β1- and α5-integrin (Int) protein levels in siCtrl- and siLRP1-treated donor PASMC. α-Tubulin served as a loading control in western blotting. Representative blots are shown. (C) Densitometry analysis of (B) (n = 4). (D) LRP1, β1 and α5 Int protein levels in cytosolic and membrane fractions of siCtrl- or siLRP1-treated donor PASMC. Representative blots are shown (n = 3). (E) Active β1 Int expression levels on cell surface of siCtrl- and siLRP1-treated donor PASMC measured by flow cytometry. The results are expressed as a mean fluorescence intensity (MFI) of active β1 Int detected with 9EG7 antibody (n = 3). (F) Proliferation of donor PASMC treated with either siCtrl or siLRP1 in the absence or presence of anti-β1 Int, anti-β4 Int, or IgG control antibody (IgG Ctrl; 10 μg/mL each) as assessed by ^{3}H-thymidine incorporation (n = 5). ns, not significant, *p < 0.05, **p < 0.01.

[37]. An imbalance between MMPs and their inhibitors is thought to contribute to the remodeling of pulmonary arteries by affecting the ECM synthesis and degradation, changing the bioavailability of growth factors, and inducing recruitment of inflammatory cells [36]. Accordingly, the inhibition of MMP activities in the hypoxic rats reduced the abundance of collagen-breakdown products in peripheral pulmonary arteries and decreased muscularization of pulmonary vessels and pulmonary arterial blood pressure thus markedly attenuating PH [35]. Since LRP1 regulates the expression of *MMP13* and *MMP14* and additionally controls mRNA levels of collagen-encoding genes (*COL11A1* and *COL15A1*), these data suggest that an increased LRP1 production in PASMC could contribute to the dysregulated synthesis and processing of ECM components and hence to de-differentiation of PASMC.

A current concept of PH pathogenesis describes a phenotypic switch of PASMC from a contractile (differentiated) to a synthetic/proliferative (de-differentiated) state. The latter is considered to drive medial thickening and thus vascular remodeling in PH [4]. According to this concept, the expression of contractile markers (α-SMA, myocardin) declines whereas cell proliferation and migration as well as production of ECM proteins (FN, collagens, OPN) increase in de-differentiated PASMC [4,18]. Although LRP1 did not promote PASMC migration, it decreased the expression of α-SMA and myocardin and elevated the production of ECM proteins as well as PASMC proliferation. These findings indicate that LRP1 does not act alone, but in concert with other factors, to facilitate the de-differentiation of PASMC. Several molecules/conditions were found to contribute to the transition of PASMC from a contractile to a synthetic state, among others PDGF-BB [38], STIM, Orai2 [39], α-enolase [40], and hypoxia [41] thus implying that a number of biological and environmental factors accompany the process of SMC de-differentiation. Noteworthy, the contractile and the synthetic phenotype of SMC represent two extremes of continuum. Between these two extremes, a high number of intermediate phenotypes, which are characterized by the selective acquisition of the features of both SMC states, exist. Thus, the increased LRP1 expression in PASMC and the cellular consequences of thereof may represent just one of the stages of the de-differentiation process. Interestingly, in PASMC isolated from IPAH lungs, LRP1 depletion did suppress cell proliferation and Col I protein expression, however, it did not affect the expression of the contractile phenotype markers. This suggests that, although LRP1 may promote the phenotypic switch of PASMC in PH, other factors are, in addition, needed to fully restore the differentiated state of PASMC [42].

Growth promoting activities of LRP1 in donor as well as IPAH PASMC were strongly dependent on the expression of β1-integrin. Altered levels of various integrins are considered to drive vascular remodeling in experimental models of PH by disturbing SMC-ECM communication [43]. For example, αvβ3-integrin was found to mediate osteoprotegerin-triggered PASMC proliferation and hence vascular remodeling of pulmonary vessel in mice exposed to hypoxia and SU5416 [44]. β3-integrin was also critical for growth, migration and ECM production of PASMC exposed to connective tissue growth factor [45]. We show for the first time the dependency of β1-integrin expression on LRP1 in PASMC and the association between β1-integrin abundance and the PASMC replication rate. These results are corroborated by the

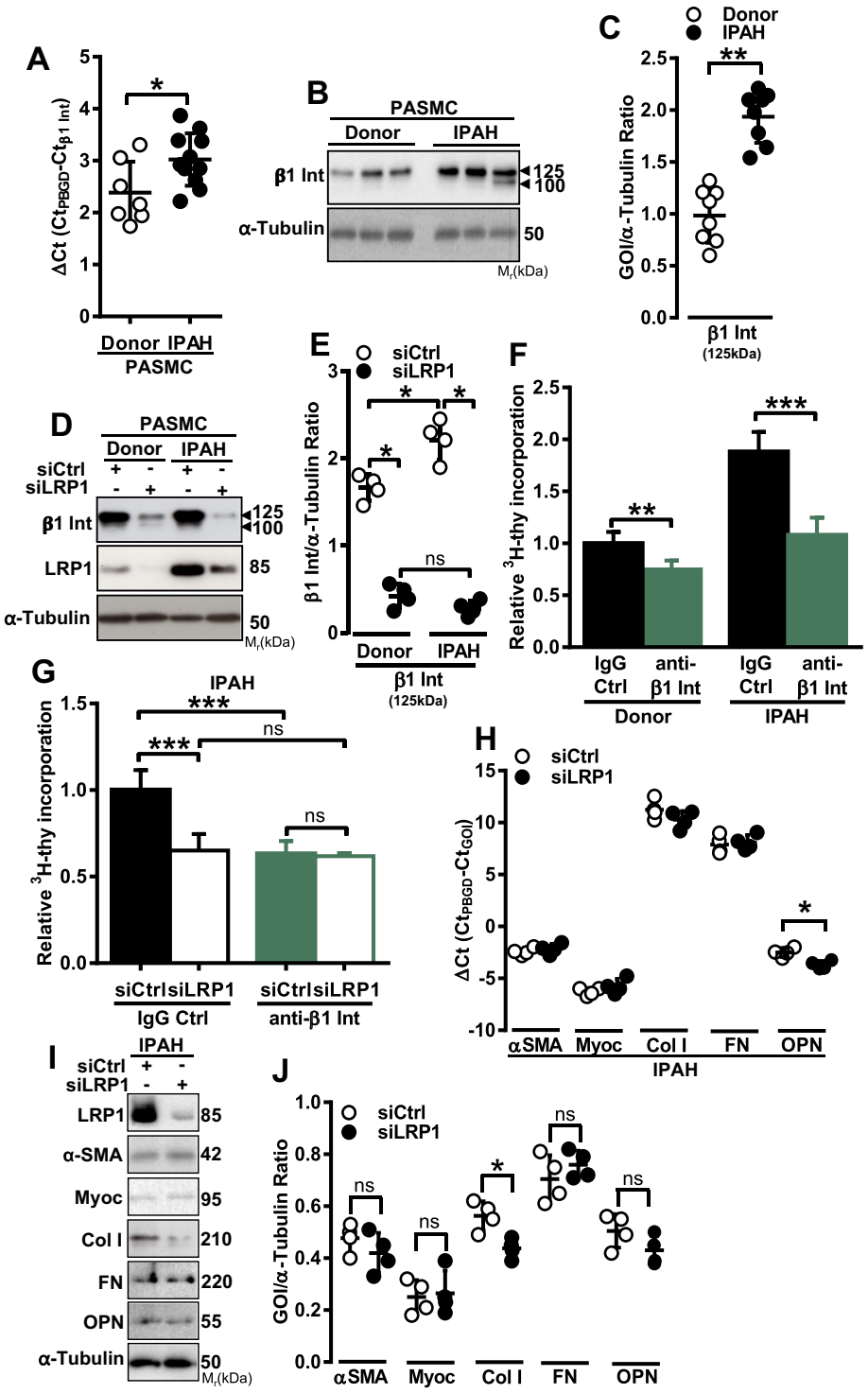

Fig. 7. LRP1 regulates proliferation of IPAH PASMC in a β1-integrin dependent manner. (A, B) β1-integrin (Int) mRNA (A) and protein (B) levels in PASMC isolated from of donors (n = 7 for RNA) and IPAH patients (n = 11 for RNA). The qPCR data are expressed as ΔCt using *PBGD* as a reference gene. For western blotting α-tubulin was used as a loading control. (C) Densitometry analysis of (B) (n = 8). (D) β1 and α5 Int protein levels in control siRNA (siCtrl)- and siRNA targeting LRP1 (siLRP1)-treated donor and IPAH PASMC. (E) Densitometry analysis of (D) (n = 4). (F) Proliferation of donor and IPAH PASMC in the absence or presence of anti-β1 Int or IgG control antibody (IgG Ctrl; 10 μg/mL each) as assessed by ^{3}H-thymidine incorporation (n = 4). (G) Proliferation of IPAH PASMC treated with either siCtrl or siLRP1 in the absence or presence of anti-β1 Int antibody or IgG Ctrl (10 μg/mL each) as measured by ^{3}H-thymidine incorporation (n = 4). (H, I) mRNA (H) and protein (I) levels of α-smooth muscle actin (α-SMA), myocardin (Myoc), collagen I (Col I), fibronectin (FN), and osteopontin (OPN) in IPAH PASMC treated with either siCtrl or siLRP1. qPCR results are expressed as ΔCt using *PBGD* as a reference gene (n = 4). Protein levels were assessed by western blotting using α-tubulin as a loading control. (J) Densitometry analysis of (I) (n = 4). ns, not significant, *p < 0.05, **p < 0.01, ***p < 0.001.

increased levels of LRP1 and β1-integrin in highly proliferating IPAH PASMC. Strikingly, previous studies highlighted the augmented α5β1-integrin levels in less differentiated SMC following injury and the inverse relationship between α5β1-integrin and α-SMA expression in SMC [46]. These findings are in line with our observation of the elevated α-SMA levels in PASMC characterized by low LRP1 abundance and hence decreased expression of β1-integrin. The direct association between β1-integrin expression and phenotypic transition of PASMC requires, however, further exploration.

Following injury, LRP1 tries to orchestrate many processes that are crucial for repairing damaged vessels. By controlling the expression of integrins, MMPs, and ECM components, it ensures proper communication of the SMC within an ever changing environment. Whether the elevated expression of LRP1 in PASMC isolated from IPAH lungs tries to compensate or rather propagates vascular damage has to be answered in future *in vivo* studies.

Transparency document

The Transparency document associated this article can be found, in online version.

Acknowledgement

We thank E. Bieniek, S. Kegel, and H. Thiele for their excellent technical assistance. The Acta2-Cre^{ERT2} mouse line was developed and kindly provided by Daniel Metzger and Pierre Chambon (Institute of Genetics and Molecular and Cellular Biology, Illkirch, Strasbourg, France).

Competing interests

None declared.

Research support

The German Research Foundation (DFG: WY119/1-3 to M.W. SFB 815, project A5, SFB 1039, project B2, SFB 1177, project C02, and SCHA 1082/6-1 to L.S.), the Else Kroner-Fresenius Foundation (to M.W.), the Cardiopulmonary Institute (CPI) (EXC 2026, Project ID: 390649896 to M.W. and L.S.) and the German Center for Lung Research (to M.W.).

References

[1] Y. Gao, T. Chen, J.U. Raj, Endothelial and smooth muscle cell interactions in the pathobiology of pulmonary hypertension, Am. J. Respir. Cell Mol. Biol. 54 (2016) 451–460.
[2] T. Stevens, S. Phan, M.G. Frid, D. Alvarez, E. Herzog, K.R. Stenmark, Lung vascular cell heterogeneity: endothelium, smooth muscle, and fibroblasts, Proc. Am. Thorac. Soc. 5 (2008) 783–791.
[3] W. Sun, S.Y. Chan, Pulmonary arterial stiffness: an early and pervasive driver of pulmonary arterial hypertension, Front. Med. 5 (2018) 204.
[4] K.R. Stenmark, M.G. Frid, B.B. Graham, R.M. Tuder, Dynamic and diverse changes in the functional properties of vascular smooth muscle cells in pulmonary hypertension, Cardiovasc. Res. 114 (2018) 551–564.
[5] D.K. Strickland, D.T. Au, P. Cunfer, S.C. Muratoglu, Low-density lipoprotein receptor-related protein-1: role in the regulation of vascular integrity, Arterioscler. Thromb. Vasc. Biol. 34 (2014) 487–498.
[6] P. Boucher, M. Gotthardt, W.P. Li, R.G. Anderson, J. Herz, LRP: role in vascular wall integrity and protection from atherosclerosis, Science 300 (2003) 329–332.
[7] L. Wujak, R.T. Bottcher, O. Pak, H. Frey, E. El Agha, Y. Chen, S. Schmitt, S. Bellusci, L. Schaefer, N. Weissmann, R. Fassler, M. Wygrecka, Low density lipoprotein receptor-related protein 1 couples beta1 integrin activation to degradation, Cell. Mol. Life Sci. 75 (2018) 1671–1685.
[8] S.C. Muratoglu, S. Belgrave, B. Hampton, M. Migliorini, T. Coksaygan, L. Chen, I. Mikhailenko, D.K. Strickland, LRP1 protects the vasculature by regulating levels of connective tissue growth factor and HtrA1, Arterioscler. Thromb. Vasc. Biol. 33 (2013) 2137–2146.
[9] L. Zhu, I. Giunzioni, H. Tavori, R. Covarrubias, L. Ding, Y. Zhang, M. Ormseth, A.S. Major, J.M. Stafford, M.F. Linton, S. Fazio, Loss of macrophage low-density lipoprotein receptor-related protein 1 confers resistance to the antiatherogenic effects of tumor necrosis factor-alpha inhibition, Arterioscler. Thromb. Vasc. Biol. 36 (2016) 1483–1495.
[10] C. Nakajima, P. Haffner, S.M. Goerke, K. Zurhove, G. Adelmann, M. Frotscher, J. Herz, H.H. Bock, P. May, The lipoprotein receptor LRP1 modulates sphingosine-1-phosphate signaling and is essential for vascular development, Development 141 (2014) 4513–4525.
[11] R.T. Schermuly, E. Dony, H.A. Ghofrani, S. Pullamsetti, R. Savai, M. Roth, A. Sydykov, Y.J. Lai, N. Weissmann, W. Seeger, F. Grimminger, Reversal of experimental pulmonary hypertension by PDGF inhibition, J. Clin. Invest. 115 (2005) 2811–2821.
[12] H. Guo, W. Liu, Z. Ju, P. Tamboli, E. Jonasch, G.B. Mills, Y. Lu, B.T. Hennessy, D. Tsavachidou, An efficient procedure for protein extraction from formalin-fixed, paraffin-embedded tissues for reverse phase protein arrays, Proteome Sci. 10 (2012) 56.
[13] G. Kwapiszewska, P. Markart, B.K. Dahal, B. Kojonazarov, L.M. Marsh, R.T. Schermuly, C. Taube, A. Meinhardt, H.A. Ghofrani, M. Steinhoff, W. Seeger, K.T. Preissner, A. Olschewski, N. Weissmann, M. Wygrecka, PAR-2 inhibition reverses experimental pulmonary hypertension, Circ. Res. 110 (2012) 1179–1191.
[14] O. Wendling, J.M. Bornert, P. Chambon, D. Metzger, Efficient temporally-controlled targeted mutagenesis in smooth muscle cells of the adult mouse, Genesis 47 (2009) 14–18.
[15] A. Rohlmann, M. Gotthardt, T.E. Willnow, R.E. Hammer, J. Herz, Sustained somatic gene inactivation by viral transfer of Cre recombinase, Nat. Biotechnol. 14 (1996) 1562–1565.
[16] B. Deng, J. Du, R. Hu, A.P. Wang, W.H. Wu, C.P. Hu, Y.J. Li, X.H. Li, MicroRNA-103/107 is involved in hypoxia-induced proliferation of pulmonary arterial smooth muscle cells by targeting HIF-1beta, Life Sci. 147 (2016) 117–124.
[17] F. Perros, D. Montani, P. Dorfmuller, I. Durand-Gasselin, C. Tcherakian, J. Le Pavec, M. Mazmanian, E. Fadel, S. Mussot, O. Mercier, P. Herve, D. Emilie, S. Eddahibi, G. Simonneau, R. Souza, M. Humbert, Platelet-derived growth factor expression and function in idiopathic pulmonary arterial hypertension, Am. J. Respir. Crit. Care Med. 178 (2008) 81–88.
[18] M. Wanjare, F. Kuo, S. Gerecht, Derivation and maturation of synthetic and contractile vascular smooth muscle cells from human pluripotent stem cells, Cardiovasc. Res. 97 (2013) 321–330.
[19] P. Moreno-Layseca, C.H. Streuli, Signalling pathways linking integrins with cell cycle progression, Matrix Biol. 34 (2014) 144–153.
[20] L. Zhou, Y. Takayama, P. Boucher, M.D. Tallquist, J. Herz, LRP1 regulates architecture of the vascular wall by controlling PDGFRbeta-dependent phosphatidylinositol 3-kinase activation, PLoS One 4 (2009) e6922.
[21] J.E. Basford, Z.W. Moore, L. Zhou, J. Herz, D.Y. Hui, Smooth muscle LDL receptor-related protein-1 inactivation reduces vascular reactivity and promotes injury-induced neointima formation, Arterioscler. Thromb. Vasc. Biol. 29 (2009) 1772–1778.
[22] J.B. Wild, P.W. Stather, N. Sylvius, E. Choke, R.D. Sayers, M.J. Bown, Low density lipoprotein receptor related protein 1 and abdominal aortic aneurysms, Eur. J. Vasc. Endovasc. Surg. 44 (2012) 127–132.
[23] L. Jiang, H. Konishi, F. Nurwidya, K. Satoh, F. Takahashi, H. Ebinuma, K. Fujimura, K. Takasu, M. Jiang, H. Shimokawa, H. Bujo, H. Daida, Deletion of LR11 attenuates hypoxia-induced pulmonary arterial smooth muscle cell proliferation with medial thickening in mice, Arterioscler. Thromb. Vasc. Biol. 36 (2016) 1972–1979.
[24] D.T. Au, Z. Ying, E.O. Hernandez-Ochoa, W.E. Fondrie, B. Hampton, M. Migliorini, R. Galisteo, M.F. Schneider, A. Daugherty, D.L. Rateri, D.K. Strickland, S.C. Muratoglu, LRP1 (low-density lipoprotein receptor-related protein 1) regulates smooth muscle contractility by modulating Ca(2+) signaling and expression of cytoskeleton-related proteins, Arterioscler. Thromb. Vasc. Biol. 38 (2018) 2651–2664.
[25] E. Revuelta-Lopez, C. Soler-Botija, L. Nasarre, A. Benitez-Amaro, D. de Gonzalo-Calvo, A. Bayes-Genis, V. Llorente-Cortes, Relationship among LRP1 expression, Pyk2 phosphorylation and MMP-9 activation in left ventricular remodelling after myocardial infarction, J. Cell. Mol. Med. 21 (2017) 1915–1928.
[26] J. Castellano, R. Aledo, J. Sendra, P. Costales, O. Juan-Babot, L. Badimon, V. Llorente-Cortes, Hypoxia stimulates low-density lipoprotein receptor-related protein-1 expression through hypoxia-inducible factor-1alpha in human vascular smooth muscle cells, Arterioscler. Thromb. Vasc. Biol. 31 (2011) 1411–1420.
[27] F.S. de Man, L. Tu, M.L. Handoko, S. Rain, G. Ruiter, C. Francois, I. Schalij, P. Dorfmuller, G. Simonneau, E. Fadel, F. Perros, A. Boonstra, P.E. Postmus, J. van der Velden, A. Vonk-Noordegraaf, M. Humbert, S. Eddahibi, C. Guignabert, Dysregulated renin-angiotensin-aldosterone system contributes to pulmonary arterial hypertension, Am. J. Respir. Crit. Care Med. 186 (2012) 780–789.
[28] J. Sendra, V. Llorente-Cortes, P. Costales, C. Huesca-Gomez, L. Badimon, Angiotensin II upregulates LDL receptor-related protein (LRP1) expression in the vascular wall: a new pro-atherogenic mechanism of hypertension, Cardiovasc. Res. 78 (2008) 581–589.
[29] P.L. Leslie, D.A. Franklin, Y. Liu, Y. Zhang, p53 regulates the expression of LRP1 and apoptosis through a stress intensity-dependent microRNA feedback loop, Cell Rep. 24 (2018) 1484–1495.
[30] R. Cal, M. Garcia-Arguinzonis, E. Revuelta-Lopez, J. Castellano, T. Padro, L. Badimon, V. Llorente-Cortes, Aggregated low-density lipoprotein induces LRP1 stabilization through E3 ubiquitin ligase CHFR downregulation in human vascular smooth muscle cells, Arterioscler. Thromb. Vasc. Biol. 33 (2013) 369–377.
[31] Y. Yamanaka, M.A. Faghihi, M. Magistri, O. Alvarez-Garcia, M. Lotz, C. Wahlestedt, Antisense RNA controls LRP1 sense transcript expression through interaction with a chromatin-associated protein, HMGB2, Cell Rep. 11 (2015) 967–976.
[32] S. Cantoni, M. Galletti, F. Zambelli, S. Valente, F. Ponti, R. Tassinari, G. Pasquinelli, N. Galie, C. Ventura, Sodium butyrate inhibits platelet-derived growth factor-induced proliferation and migration in pulmonary artery smooth muscle cells through Akt inhibition, FEBS J. 280 (2013) 2042–2055.
[33] S.C. Muratoglu, I. Mikhailenko, C. Newton, M. Migliorini, D.K. Strickland, Low density lipoprotein receptor-related protein 1 (LRP1) forms a signaling complex with platelet-derived growth factor receptor-beta in endosomes and regulates activation of the MAPK pathway, J. Biol. Chem. 285 (2010) 14308–14317.
[34] E. Loukinova, S. Ranganathan, S. Kuznetsov, N. Gorlatova, M.M. Migliorini, D. Loukinov, P.G. Ulery, I. Mikhailenko, D.A. Lawrence, D.K. Strickland, Platelet-derived growth factor (PDGF)-induced tyrosine phosphorylation of the low density lipoprotein receptor-related protein (LRP). Evidence for integrated co-receptor function between LRP and the PDGF, J. Biol. Chem. 277 (2002) 15499–15506.
[35] A.L. Frump, M.E. Albrecht, J.N. McClintick, T. Lahm, Estrogen receptor-dependent attenuation of hypoxia-induced changes in the lung genome of pulmonary hypertension rats, Pulm Circ 7 (2017) 232–243.
[36] J. Herget, J. Novotna, J. Bibova, V. Povysilova, M. Vankova, V. Hampl, Metalloproteinase inhibition by Batimastat attenuates pulmonary hypertension in chronically hypoxic rats, Am. J. Physiol. Lung Cell. Mol. Physiol. 285 (2003) L199–L208.
[37] H. Lepetit, S. Eddahibi, E. Fadel, E. Frisdal, C. Munaut, A. Noel, M. Humbert, S. Adnot, M.P. D'Ortho, C. Lafuma, Smooth muscle cell matrix metalloproteinases in idiopathic pulmonary arterial hypertension, Eur. Respir. J. 25 (2005) 834–842.
[38] C. Xie, Y. Guo, T. Zhu, J. Zhang, P.X. Ma, Y.E. Chen, Yap1 protein regulates vascular smooth muscle cell phenotypic switch by interaction with myocardin, J. Biol. Chem. 287 (2012) 14598–14605.
[39] R.A. Fernandez, J. Wan, S. Song, K.A. Smith, Y. Gu, M. Tauseef, H. Tang, A. Makino, D. Mehta, J.X. Yuan, Upregulated expression of STIM2, TRPC6, and Orai2 contributes to the transition of pulmonary arterial smooth muscle cells from a contractile to proliferative phenotype, Am. J. Physiol. Cell Physiol. 308 (2015) C581–C593.

[40] J. Dai, Q. Zhou, J. Chen, M.L. Rexius-Hall, J. Rehman, G. Zhou, Alpha-enolase regulates the malignant phenotype of pulmonary artery smooth muscle cells via the AMPK-Akt pathway, Nat. Commun. 9 (2018) 3850.
[41] F. Wang, X. Xu, W. Tang, L. Min, J. Yang, Rab6A GTPase contributes to phenotypic modulation in pulmonary artery smooth muscle cells under hypoxia, J. Cell. Biochem. (2018).
[42] K. Lehti, N.F. Rose, S. Valavaara, S.J. Weiss, J. Keski-Oja, MT1-MMP promotes vascular smooth muscle dedifferentiation through LRP1 processing, J. Cell Sci. 122 (2009) 126–135.
[43] A. Umesh, O. Paudel, Y.N. Cao, A.C. Myers, J.S. Sham, Alteration of pulmonary artery integrin levels in chronic hypoxia and monocrotaline-induced pulmonary hypertension, J. Vasc. Res. 48 (2011) 525–537.
[44] D. Jia, Q. Zhu, H. Liu, C. Zuo, Y. He, G. Chen, A. Lu, Osteoprotegerin disruption attenuates HySu-induced pulmonary hypertension through integrin alphavbeta3/FAK/AKT pathway suppression, Circ Cardiovasc Genet, 10, (2017).
[45] G. Li, Y. Hu, P. Jia, J. Fu, C.X. Lu, Y.Q. Sun, B. Liu, [Integrin beta3 pathway mediated connective tissue growth factor-induced proliferation, migration and extracellular matrix deposition of pulmonary arterial smooth muscle cells], Zhonghua Er Ke Za Zhi, 49 (2011) 895–900.
[46] J.G. Pickering, L.H. Chow, S. Li, K.A. Rogers, E.F. Rocnik, R. Zhong, B.M. Chan, alpha5beta1 integrin expression and luminal edge fibronectin matrix assembly by smooth muscle cells after arterial injury, Am. J. Pathol. 156 (2000) 453–465.